

Ultra-high-field 7T *in vivo* normative atlas of the hippocampal subfields using susceptibility weighted imaging

Maged Goubran¹, Brendan Santyr¹, Dave Rudko¹, Joe Gati¹, Trevor Szekeres¹, Terry M. Peters¹, and Ali R. Khan¹
¹Robarts Research Institute, London, Ontario, Canada

Introduction

The hippocampus and its substructures are of great importance in the pre-operative evaluation of intractable epilepsy [1]. Recent advances in ultra-high-field imaging provide the opportunity to study hippocampal sub-regions *in-vivo* at high resolution. Previous studies [2] have focused on standard T₂-weighted sequences to attain the necessary contrast and resolution to delineate the hippocampal subfields and investigate morphometric properties. Quantitative MRI sequences [3] have the added benefit of providing additional information, such as T₂* relaxation time and quantitative volume magnetic susceptibility of hippocampal substructures. These quantitative metrics can be used to better characterize the structures of interest while still allowing use of traditional volumetric and morphometric analysis. To this end, our objective is to develop a normative atlas using 7T quantitative susceptibility imaging and evaluate its use in investigating hippocampal sub-structures for use in voxel-based and morphometric studies.

Methods

Materials & Imaging: The subject cohort included eighteen healthy controls (10 Males, 8 Females, mean age 31.3 ± 8.7). A 16 channel head coil was used for imaging on a 7 Tesla 7T680 Head Only Magnet (Agilent, Santa Clara, CA, U.S.A/ Siemens, Erlangen, Germany). The imaging sequence used for this study was a multi-echo gradient-echo sequence with six echoes and a 0.5 mm in-plane resolution (TR=40 ms, TE=4.57 ms, Echo spacing= 4.89 ms, flip angle=13°, N=1, matrix=256x360x80, slice thickness= 1.5 mm, FOV=128x180x120 mm). From the gradient echo data, susceptibility-weighted, R₂*, local frequency shift (LFS) and quantitative susceptibility (QS) maps were reconstructed. Specifically, channel combination and removal of channel dependent phase offsets were performed using the hermitian product method. The resulting raw phase images were spatially unwrapped and the residual slowly-varying background phase was removed by applying a Gaussian high-pass filter. SW images were then calculated using the LFS map and a magnitude image created by averaging the magnitude images of all echoes. R₂* maps were generated from the bias-field corrected magnitude data using a Levenberg-Marquart least squares fitting routine.

Labeling protocol: The manual hippocampal subfield delineation protocol [1] has been adapted and modified to include new subfield boundaries revealed by the 7T MRI. The hippocampus was partitioned into anterior (head), posterior (tail), and mid-region (body), where the following sub-regions were segmented; Subiculum (SUB), Ammon's horn (CA1-CA3), and CA4+Dentate Gyrus (DG). To assess the accuracy and reproducibility of our segmentation protocol, five volunteers were segmented a second time by a separate operator and the resulting labels compared to the first segmentation using the dice similarity coefficient (DSC), and the absolute percentage volume error ($|\delta V_p|$).

Template construction: To generate an average atlas we constructed a template using iterative groupwise diffeomorphic registration as implemented in the ANTS software [4]. Bias-corrected images were first affine registered to a single subject and averaged to create an initial template. Then geodesic diffeomorphic registration using a symmetric normalization (GreedySYN) transformation was used to register all the images to this template resulting in an updated average, and this process is iterated while allowing greater deformations at each step. After template construction, the R₂*, LFS, SWI, QS maps, as well as the segmented labels of each subject were warped to the atlas space, upsampled to 0.5 mm isotropic resolution and averaged, using majority vote to fuse the labels.

Results

Table 1 summarizes the volumes and R₂* values of the atlas labels on the quantitative maps. The difference between quantitative intrinsic MR measures of adjacent subfields, such as R₂* difference between the Subiculum, CA1 and CA2/CA3, demonstrate the feasibility of performing quantitative voxel based analysis using our atlas. Figure 1 shows models of the subfield labels and their precise alignment on the average atlas. The inter-rater reliability results are summarized in Table 2. The dice metric was lower for the smaller subfields as expected due to the bias of the measure towards bigger structures. Both the dice metric and volume difference measures (in mm³) demonstrate, on average, high agreement between both raters across the subfields, which validates the repeatability of our protocol. It is however more difficult to compare our subfield volumes with previous attempts of hippocampal subfield volumetry due to the underlying differences in the delineation protocols.

Table1: Subfield volumes and R₂* values on the average atlas

	Volume (mm ³)	R ₂ * (1/s)
	Mean	Mean (Std)
Sub	195.5	32.3 (4.7)
CA1	272.9	25.7 (3.7)
CA2 + CA3	70.5	31.1 (3.3)
CA4+DG	256.4	29.5 (5.0)
Hp tail	366.4	28.2 (3.9)
Hp head	1412.1	30.1 (4.6)

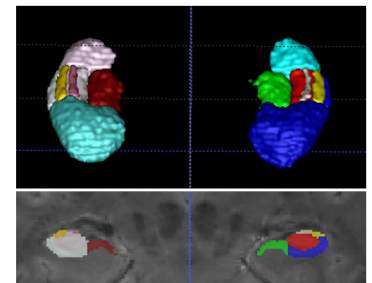


Figure 1. Top: Models of the atlas subfield segmentations. Bottom: Segmentation labels overlaid on the average magnitude of echoes.

Table2: dice similarity coefficient and absolute percentage volume error metrics

		Sub	CA1	CA2+CA3	CA4+DG	Hp tail	Hp head	Total
DSC	L	0.605	0.714	0.638	0.801	0.692	0.768	0.839
	R	0.734	0.796	0.682	0.847	0.706	0.814	0.844
$ \delta V_p $		9.6	6.0	11.3	11.2	15.4	6.7	6.5

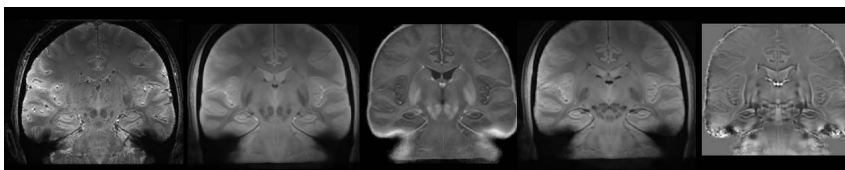
Conclusion

We constructed a normative atlas of the hippocampal subfields from *in vivo* SW images of eighteen healthy volunteers on 7T MRI. Using our reliable manual delineation protocol of the subfields, we demonstrated the feasibility of using

our atlas in voxel based and morphometry analysis of the hippocampus. This work can be complemented by further applying pre-operative patient-specific analyses using the created atlas to assess and localize structural and functional abnormalities in diseases as intractable epilepsy.

References

- [1] Mueller et al. *Epilepsia* (2009) vol. 50 (6) pp. 1474-83 2009 [2] Wisse et al. *Neuroimage* (2012) vol. 61 (4) pp. 1043-9 [3] de Rochefort et al. *Magnetic Resonance in Medicine* (2010) vol. 63 pp. 194 - 206. [4] Avants et al. *Neuroimage* (2004) vol. 23 Supp (1) pp. S139-S150



Avg. mag. of echoes Single subject Avg. mag. of echoes Atlas R2* Map SWI Map QS Map

Figure2. Single subject as well as atlas-based images of (i) average magnitude across echoes, (ii) R₂*, (iii) qualitative SWI and (iv) QS maps